Solidification Processing of Reduced Graphene Oxide Dispersed Aluminum Composites by Squeeze Casting

A.G. Arsha
CSIR-National Institute for Interdisciplinary Science and Technology, Trivandrum, India
Academy of Scientific and Innovative Research (AcSIR), Ghaziabad-201002, India
Omid Ghaderi
University of Wisconsin-Milwaukee, Wisconsin, USA
T.P.D. Rajan
CSIR-National Institute for Interdisciplinary Science and Technology, Trivandrum, India
Academy of Scientific and Innovative Research (AcSIR), Ghaziabad-201002, India
P.K. Rohatgi
University of Wisconsin-Milwaukee, Wisconsin, USA

ABSTRACT

This paper is on the processing of Al (A356) reduced graphene oxide (rGO) composites by the squeeze casting technique to obtain improved mechanical and thermal properties. Reduced graphene oxide, a two-dimensional carbon allotrope with very-high mechanical properties and thermal conductivity is used as a reinforcement in A356 aluminum alloy. Graphite was initially converted to rGO using the Hummer's method. A hybrid method was employed to produce rGO-reinforced A356 alloy matrix composites (incorporating 0.3 to 0.75wt.% rGO) by applying mechanical stirring in a semisolid state followed by squeeze casting for uniform dispersion. Squeeze pressure was crucial for increasing the cooling rate to produce a finer microstructure and eliminate porosity. Reduced graphene oxide was uniformly dispersed within the A356 alloy matrix by applying both mechanical stirring for dispersion and squeeze pressure for rapid solidification and pore free casting. The squeeze cast A356-0.5% rGO composites after T6 heat treatment had an increase in tensile strength from 260 MPa to 346 MPa, an increase in hardness 106 BHN to 130 BHN, and a reduction in coefficient of thermal expansion (CTE) from 21.7 ×10-6/°C to 10.8 ×10-6/°C, at RT-50C (122F). These results suggest potential applications of these composites in high performance industrial, automotive, and aerospace sectors.

Keywords: reduced graphene oxide, rGO, squeeze casting, aluminum, composites, mechanical stirring

INTRODUCTION

Metal matrix composites (MMCs) are alternative materials for automotive and aerospace sectors since MMCs have high specific strength and specific modulus which enables lighter components with a lower coefficient of thermal expansion and improved wear resistance.[1-3] Powder metallurgy and metalcasting are typically, the methods employed for the synthesis of aluminum composites for incorporating reinforcements to improve properties.[4,5] Carbon nanotubes and graphene, have received attention as potential reinforcements in MMCs because of their exceptionally high mechanical and thermal properties. Graphene, with its distinctive two-dimensional structure, also has a higher specific surface area and enhanced load transfer efficiency. Consequently, incorporating graphene provides a promising avenue to enhance the stiffness, strength, and conductivity of aluminum composites. However, synthesis of Al-graphene composites faces two critical challenges, first, achieving uniform dispersion of graphene in Al is hindered by agglomeration due to Van der Waals forces, which leads to the formation of clusters. Second, the interface between graphene and Al tends to be weak due to the poor wettability of carbon by molten metal and the tendency for the formation of aluminum carbide. Reduced graphene oxide (rGO) is a viable alternative to pristine graphene as a reinforcement in aluminum matrix composite materials.[6] Since it is lower in cost and possesses high hydrophilicity allowing stable aqueous colloids, and it may form stronger interfaces with Al due to functional groups in its surfaces.

Consequently, recent research efforts have investigated developing Al/rGO composites using graphite as a precursor.[7] Zan et al[8] conducted research focusing on achieving uniform dispersion of graphene oxide within aluminum powder through direct electrostatic adsorption. Their findings indicated an 18% enhancement in elastic modulus compared to unreinforced aluminum. This study explored the impact of graphene additives on the mechanical properties of aluminum using the powder metallurgy technique. In a prior study, an Al/graphene composite was developed by incorporating 0.3 wt% of graphene nanoparticles.[9] The research involved a multistep experimental procedure, and the resultant composite exhibited a tensile strength of no more than 249 MPa.[9]

Powder metallurgy and metalcasting are commonly used to synthesize advanced Al-matrix composites with exceptional mechanical, thermal, and tribological properties.[10] These traditional methods for producing aluminum-carbon composite materials face challenges due to the substantial difference in the densities of carbon and aluminum, as well as the limited affinity of carbon for molten aluminum. Consequently, these methods often result in composite materials with inferior properties. To develop high-performance Al-matrix composites with a favorable combination of high strength and acceptable ductility, this study achieved the synthesis of bulk nanostructured aluminum/rGO composites through a combination of stir mixing in semisolid state followed by the squeeze casting process.[11]

EXPERIMENTAL PROCEDURES

PREPARATION OF rGO

Reduced graphene oxide was synthesized from graphite particles by using the Hummer's method,[12] which is a common chemical oxidation method to synthesis graphene oxide (GO) from graphite shown in Figure 1.

Figure 1. Synthesized graphene oxide and reduced graphene oxide.

Hummer's Method for preparation of graphene oxide from graphite

Hummer's Method[13] is a widely recognized approach to obtain GO from graphite powder. Graphene oxide serves as an essential precursor for the preparation of reduced graphene oxide (rGO) or other functionalized graphene material, Figure 2. Ten grams of high-quality graphite powder is mixed with 5 grams of sodium nitrate ($NaNO_3$) and then 220 grams of concentrated sulfuric acid (H_2SO_4) is slowly added to the graphite powder and sodium nitrate mixture. The addition of sulfuric acid is carried out by stirring in an ice bath to maintain a controlled temperature. Once the sulfuric acid has been added, 30 grams of potassium permanganate ($KMnO_4$) is carefully introduced into the solution. During this step, it is crucial to keep the temperature below 20C (68F) to ensure a controlled reaction. After the addition of $KMnO_4$, the mixture is stirred at room temperature for a specific duration to promote the oxidation of graphite. Subsequently, the temperature is increased to 40C (104F), which accelerates the reaction kinetics. Following the temperature increase, 300 ml of water is added to the solution, leading to a reduction in the reaction temperature. To control the progress of the reaction, the solution is further stirred for 90 minutes at 90°C (194F) to facilitate the completion of the chemical reaction. This ensures the conversion of graphite into graphene oxide. To neutralize any remaining potassium permanganate, hydrogen peroxide (H_2O_2) is added to the solution. This step is essential to prevent unwanted reactions and ensure the purity of the obtained graphene oxide. The resulting graphene oxide suspension is then subjected to centrifugation to separate the solid graphene oxide from the liquid phase. After centrifugation, the obtained graphene oxide is dried at room temperature.

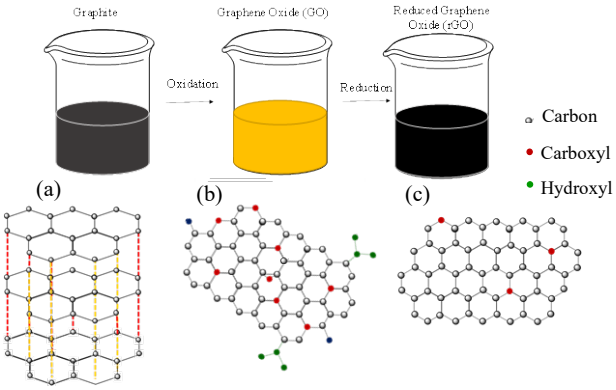

Figure 2: Representation of the (a) graphite, (b) graphene oxide (GO) and (c) Reduced graphene oxide (rGO) production process and chemical structure.

Modified Hummer's method for synthesis of rGO

Graphene oxide is a highly versatile material that can be further reduced to obtain reduced graphene oxide (rGO) or even pristine graphene. The reduced graphene oxide or graphene obtained after reduction has improved electrical and mechanical properties compared to graphene oxide, making it suitable for many applications in electronics, sensors, and composites.[14] The two commonly used chemical reducing agents are hydrazine and sodium borohydride. Figure 2 shows a representation of the graphite, GO and rGO production process and chemical structure.

Hydrazine which is a powerful reducing agent that was used to reduce graphene oxide. The process involves the addition of 0.1 µl hydrazine to the graphene oxide ((1g) + 1liter water), followed by gentle heating for 1 hour. Hydrazine donates electrons to the oxygen-containing functional groups in GO, converting them to water vapor and nitrogen gas, while simultaneously reducing the carbon atoms.[15] Finally, 10 mg $NaBH_4$ is added to the solution and refluxed for 36 hrs. Sodium borohydride donates electrons to the oxygen functional groups, leading to their removal and the restoration of sp^2 carbon-carbon bonding.[16]

PREPARATION OF Al-rGO COMPOSITES

Synthesized rGO was successfully incorporated into A356 alloy using a combination of modified stir mixing in a semisolid state and squeeze casting techniques. Combined semisolid state mixing and squeeze casting shown in Figure 3 combines the properties of these two distinctive techniques. In the semisolid mixing step, the metal was completely melted to 700C (1292F), the molten metal was skimmed, and one percent magnesium was added. The molten metal was slowly cooled to the semisolid temperature range of 585-595C (1085-1103F). A mechanical stirrer was introduced to the semisolid slurry with a stirring rate of 300 rpm during this incorporation process. The preheated rGO powder at 150C (302F) was introduced into the molten semisolid slurry of A356 alloy. Stir mixing while in the semisolid state helped in the dispersion of rGO platelets due to higher viscosity. The rGO content added to the aluminum alloy ranged from 0.3 to 0.75 wt.%. To improve the wettability between the graphene particles and the Al matrix, 1 wt.% pure magnesium was introduced into the molten metal. Stirring at the same rate continued for 5 minutes after adding all the particles to the melt. Subsequently, the temperature of the melt was raised to its liquidus state, and the liquid metal was stirred for an additional 5 minutes at this temperature just before pouring. The composite melt was then solidified using the squeeze casting technique with a 25T hydraulic press. which was performed above the liquidus temperature of the matrix material, reaching approximately 720C (1328F). For comparison purposes, molten A356 alloy without rGO was also subjected to the same casting procedure. Both the reinforced composite and the alloy were later given a T6 heat treatment, involving solution treatment at 540C (1004F) for 6 hours followed by an age hardening process at 160C (320F) for 6 hours.

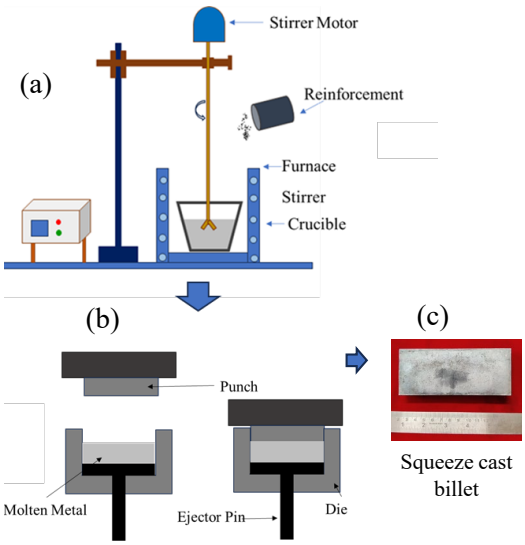

Figure 3. Schematic diagram of (a,b) combined stir mixing and squeeze casting process (c) squeeze cast billet.

STRUCTURE AND MORPHOLOGY OF SYNTHESIZED GRAPHENE OXIDE AND REDUCED GRAPHENE OXIDE

Figure 4 shows the scanning electron microscopy (SEM) and energy dispersive X-ray spectroscopy (EDS) views of the graphite, GO and rGO particles. The graphite exhibits a large flaky texture and a layered microstructure. The SEM image of reduced graphene oxide also shows a plate-like or flaky shape, similar to graphene oxide. However, in rGO the flakes are typically more crumpled and wrinkled due to the reduction process, possibly due to the removal of oxygen-containing functional groups from graphene oxide. The reduction process results in the restoration of the sp_2 carbon network in rGO leading to a more graphene-like structure. As a result, while rGO retains the layered microstructure of graphene, it has some irregularities in the flakes, giving it a wrinkled appearance as observed in Figure 4h.[17] The rGO is finer in size compared to graphene oxide which may be due to the breakage of bond during the reduction process. The EDS technique showed that graphite had a predominant atomic composition of 96.76% carbon (C) and 3.24% oxygen (O). Graphene oxide exhibited 64.28% carbon (C) and 35.72% oxygen (O). Reduced graphene oxide had 78.20% carbon (C) and 21.80% oxygen (O), however the carbon contents determined by EDS are not quantitatively accurate. Graphite is a conductor of heat and electricity.

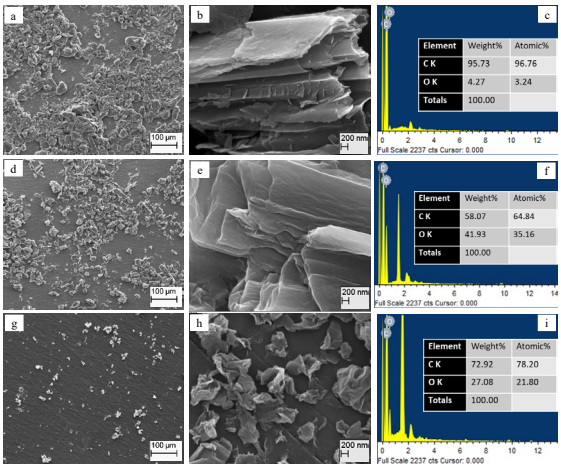

Figure 4. SEM micrograph and EDS of (a, b, c) graphite (d, e, f) graphene oxide (g, h, i) Reduced graphene oxide

Figure 5 shows the transmission electron microscopy (TEM) images of graphene oxide (GO) and reduced graphene oxide (rGO), and both images display a sheet-like morphology. In the TEM images, the two-dimensional layered nature of graphene is visible. The sheets exhibit some degree of wrinkling and corrugation, especially in the case of GO due to the presence of oxygen functional groups. The sheet-like morphology of both graphene oxide and reduced graphene oxide is expected to help with reinforcement in composites due to increased surface area for load transfer.

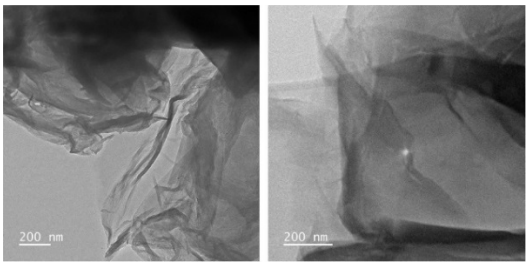

Figure 5. A TEM image of (a) graphene oxide (b) reduced graphene oxide.

In Raman Spectroscopy the extent of the disorder is typically assessed through the intensity ratio (I) of the disorder-induced D band to the Raman-allowed G band, referred to as I_D/I_G. Figure 6 shows the Raman spectra of graphene oxide, reduced graphene oxide (rGO), and the base material graphite. For graphite, the D band appears at 1331 cm,$^{-1}$ while for rGO, it occurs at 1328 cm.$^{-1}$ The G band is consistent among all sp^2 carbon forms and emerges from the stretching of the C-C bond. This band is a product of first-order Raman scattering.[18] The increase in the I_D/I_G ratio, transitioning from 0.1 for graphite to 0.84 for rGO, suggests the incorporation of oxygen-containing functional groups into the graphitic planes. A high I_D/I_G ratio indicates that the reduced graphene oxide sample is highly disordered, while a low I_D/I_G ratio indicates that the rGO sample is highly ordered.[19] This elevated I_D/I_G ratio in rGO compared to graphite indicates the formation of smaller sp^2 domains during reduction, contrasting with the larger domains found in graphite. The 2D band at 2489 cm^{-1} indicates that the rGO is mostly composed of few layered graphene sheets. The frequency of the 2D band is typically around 2670 cm,$^{-1}$ but it can shift to lower frequencies in rGO due to the presence of oxygen functional groups. A sharp peak at ~2489 cm^{-1} indicates that the oxygen functional groups have been reduced, which is a sign of high-quality rGO.

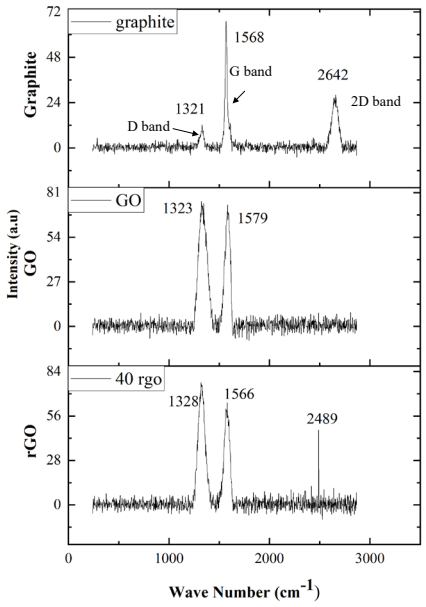

Figure 6. Raman spectra of graphite and synthesized rGO.

The graphite, GO, and rGO, the crystal phase and interlayer spacing were investigated using XRD spectra and are displayed in Figure 7. One distinct peak is seen for graphite at 2θ = 26.62.° The two peaks for GO were observed to be moved to 9.03,° indicating complete oxidation of the graphite into GO.[20] This rise in value was induced by the intercalation of oxide functional groups, including hydroxyl, carbonyl, and carboxyl groups, onto the carbon basal plane through chemical oxidation reactions. As a result, there was an increase in the spacing between adjacent carbon layers. The peak for RGO at 2θ = 24.10° is wider because oxygen-containing functional groups were greatly reduced during the chemical reduction.[19] Furthermore, the d-spacing of rGO was reduced from 0.9794 nm to 0.3689 nm, indicating the successful removal of oxygen-containing functional groups. This reduction also demonstrated that the thick layers formed by stacking rGO nanosheets on top of each other were a result of the strong Van der Waals interactions between individual layers.[21] At 2θ = 42.60° a second, small peak can be seen, and it is due the presence of disordered carbon compounds.

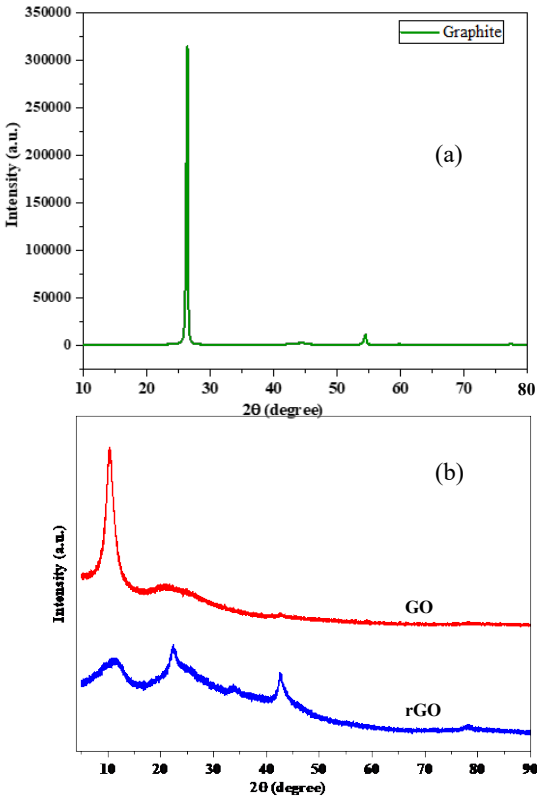

Figure 7. Shows the XRD plot of (a) graphite (b) graphene oxide and reduced graphene oxide.

Figure 8 presents the Fourier transform infrared spectroscopy (FTIR) spectra of graphite, GO, and rGO. At the outset, the FTIR spectra of graphite displayed an absence of significant peaks, highlighting the inherent chemical inertness of bulk graphite.[12] In contrast, the FTIR spectra of graphene oxide (GO) exhibited the presence of several functional groups.

Specifically, a prominently intense band at 3329 cm^{-1} was attributed to the O–H stretching vibration, signifying the inclusion of OH and COOH functional groups within the GO structure.[19,22] Additionally, distinctive peaks corresponding to the carbonyl C=O stretching vibration at 1721 $cm,^{-1}$ the C–C stretching vibration characteristic of unoxidized graphitic domains at 1613 $cm,^{-1}$ the O–H deformation at 1404 $cm,^{-1}$ the C–O stretching associated with epoxy groups at 1217 $cm,^{-1}$ and the C–O stretching vibration attributed to alkoxy groups at 1051 cm^{-1} were observed.[23]

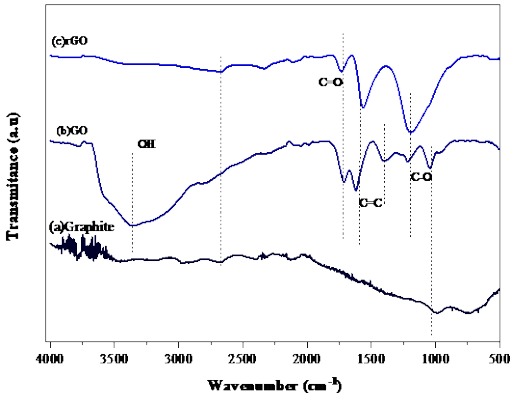

Figure 8. FTIR spectra of (a) graphite (b) GO and (c) reduced graphene oxide.

However, in the FTIR spectra of reduced graphene oxide (rGO), the O–H stretching vibration peak, originally present in GO, was notably absent. This absence is due to the reduction-induced removal or modification of the hydroxyl groups during the transformation from GO to rGO, a crucial characteristic of the reduction process that is significant for various applications of graphene-based materials. The FTIR findings agree with the result of the prior research.[24] confirming chemical transformations that took place during the creation of rGO from graphite.

PROCESSING AND CHARACTERIZATION OF A356-RGO COMPOSITE

The microstructure of the T6 heat-treated A356 alloy has been shown in Figure 9 (a, c). This picture consists of eutectic Al and Si particle phases. In the base A356 alloy, the secondary dendrite arm spacing (SDAS) is of the order of 37 µm for squeeze cast samples. The microstructure of the heat-treated A356-0.5 rGO composite shows a significant refinement in the SDAS around 15 microns in size suggesting that the SDAS is getting reduced due to the presence of rGO. The finer microstructure is advantageous as it can contribute to improved mechanical properties, including increased strength and toughness.[23] The SEM elemental mapping shown in Figure 10 also confirms the absence of aggregation or clumping of rGO within the Al matrix. The mapping also reveals the uniform distribution of carbon in the Al matrix.

The addition of increasing amount of rGO in the matrix A356 alloy reduces the coefficient of thermal expansion (CTE) of A356-0.5rGO composite (Figure 11). The CTE of the composites decreased from 21.7 to 10.8 $\times 10^{-6}$ /°C at RT-50C (122F), and similar decreases in CTE are observed until 200C (392F).[25-27]

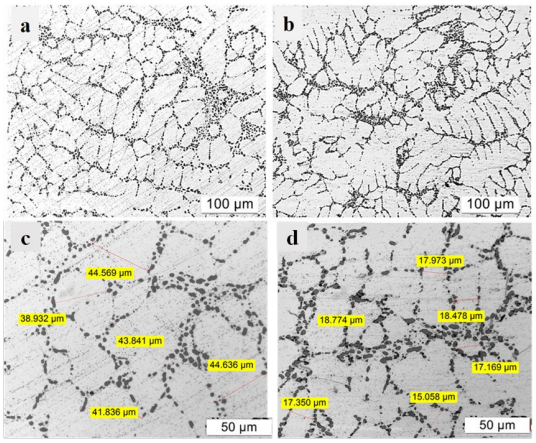

Figure 9. Microstructure of heat treated (a & c) A356 alloy and (b & d) A356- 0.5wt.% rGO composite of varying magnification.

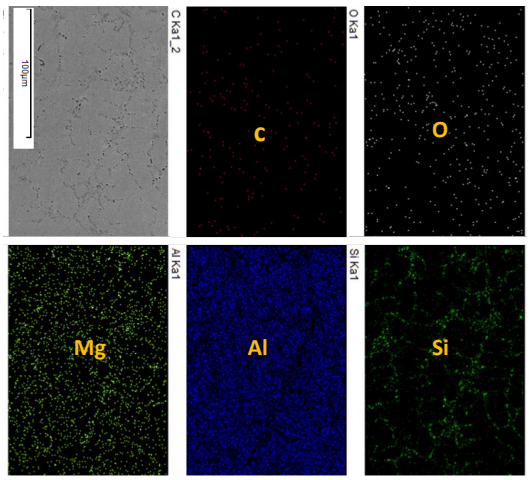

Figure 10. SEM Elemental mapping of 0.5wt.% Al-rGO composite.

In the 0.5wt% GO composite, the interface area is large, and this can further help to reduce the CTE.[28,29] In composites with higher concentrations (0.75wt.%), agglomeration of the reinforcing phase may occur. When rGO particles clump together, they may not be able to contribute to the reduction of the CTE. This can result in higher CTE values. Figure 12 illustrates the improvement in the hardness of the A356 alloy achieved through the addition of rGO in the T6 condition. The rGO content for maximum hardness is in the range of 0.3-0.5 wt.%. Apparently, at this concentration, the rGO platelets were dispersed uniformly in the alloy matrix and were able to provide maximum reinforcement. The increase in hardness is likely to be due to dispersion of rGO and refinement of microstructure. Grain refinement improves simultaneously the strength and plasticity of metallic materials according to Hall-Petch equation.[30] Smaller grains could lead to an increase in the hardness of the material.

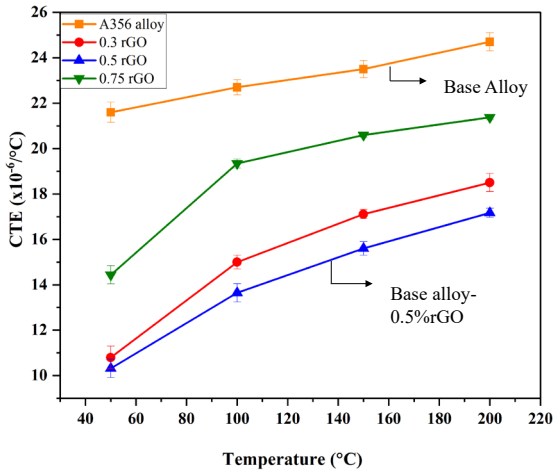

Figure 11. CTE A356 alloy and A356-rGO composites at T6 heat treated condition.

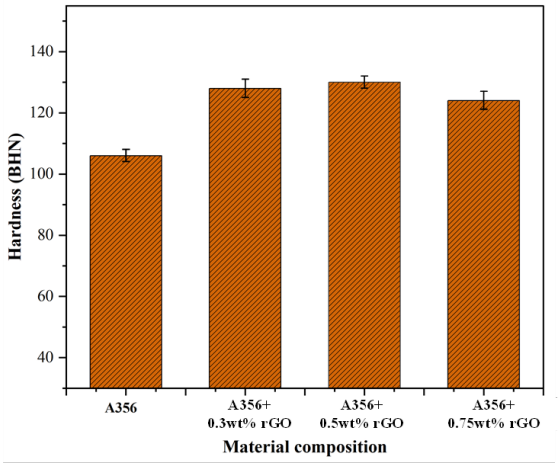

Figure 12. Brinell hardness of A356 alloy and rGO composites in T6 condition.

However, a further increase in rGO content to 0.75% leads to a decrease in hardness possibly due to the agglomeration of the rGO platelets. When the rGO content was too high, apparently the platelets started to cluster together, forming large aggregates resulting in a decrease in hardness.

Figure 13a shows the representative engineering stress-strain curves of the squeeze cast Al-rGO composites containing 0.3 to 0.75 wt.% rGO, together with the tensile response of reinforced Al matrix cast using squeeze casting. The incorporation of 0.5wt.% reduced graphene oxide (rGO) into the A356 alloy resulted in significant enhancements in its mechanical properties. The ultimate tensile strength (UTS) of the base A356 alloy increased from 260 ± 3 MPa to 346 ± 4 MPa. This enhancement can be attributed to the reinforcing effect of rGO, apparently a strong interfacial bonding between rGO and the aluminum matrix effectively transfers stress, resulting in improved UTS.[31]

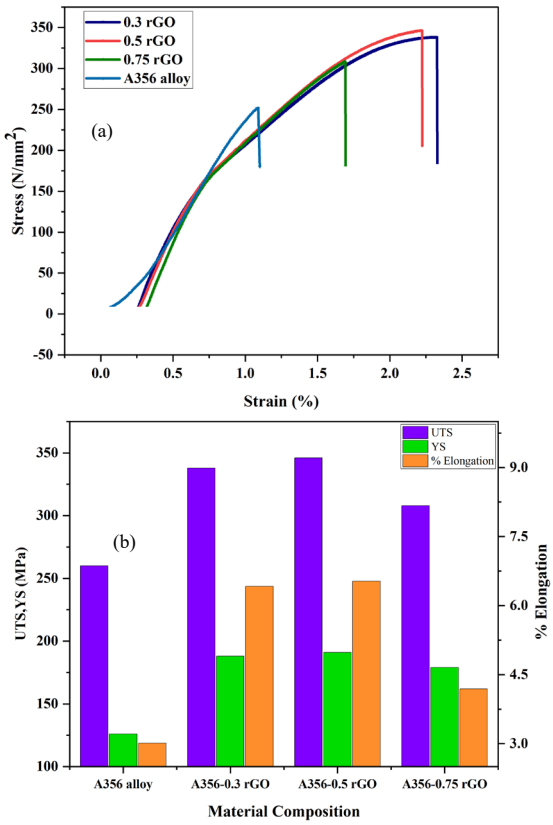

Figure 13. (a) Stress-strain curve (b) UTS, YS and elongation of A356 alloy and rGO composite.

Additionally, the yield strength of the A356 alloy increased from 125 ± 0.5 MPa to 191 ± 1 MPa as a result of incorporation of rGO is shown in Figure 13b.Yield strength represents the point at which a material begins to deform plastically, and this enhancement indicates increased resistance to plastic deformation.[32,33]

Furthermore, the percentage elongation of the composite increased from 3.1% to 6.53%, this signifies an improvement in the ability of the material to deform plastically before fracture, which is crucial for applications requiring ductility. The increase in percentage elongation suggests that the incorporation of rGO has not only improved strength but also ductility.[6]

The rGO composites exhibited improved ductility when compared to previously reported Al/graphene composites in the literature.[34,35] This indicates that the composite maintains its ability to deform before failure, despite the increase in strength. These improvements can be attributed to the reinforcing effects of rGO, which strengthens the material and enhances its ability to withstand mechanical loads.[36] These results clearly indicate that rGO is an effective reinforcement in the Al matrix.[37,38] and Al-rGO composites can find applications in the aerospace and automotive sectors.

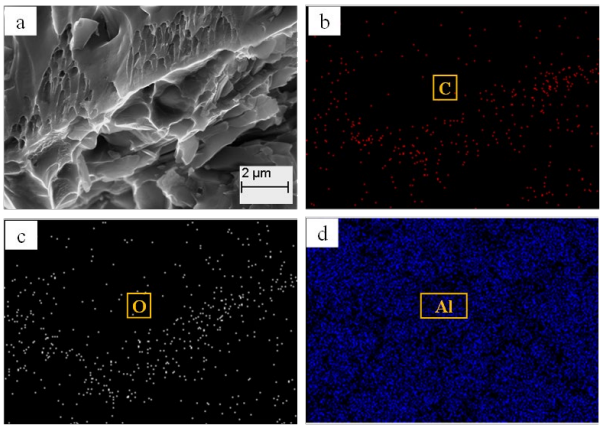

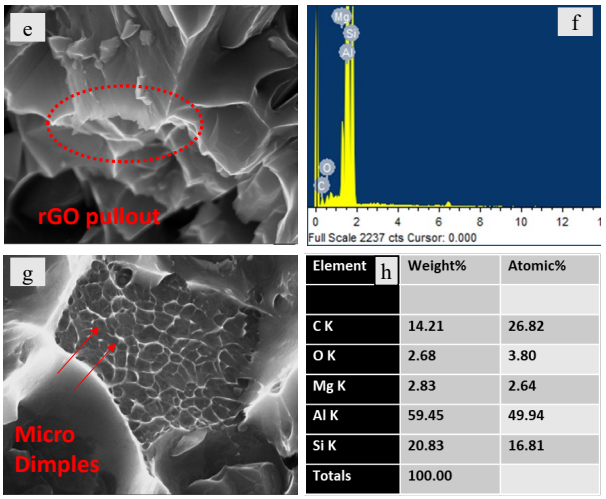

h

Element	Weight%	Atomic%
C K	14.21	26.82
O K	2.68	3.80
Mg K	2.83	2.64
Al K	59.45	49.94
Si K	20.83	16.81
Totals	100.00	

Figure 14 (a-d). SEM elemental mapping of the tensile fracture surface. Views (e, g) show the tensile fracture surface and views (f,h) shows the EDS of the Al-0.5wt.% rGO composite.

The SEM photographs and elemental mapping of the fracture surface morphology of composites incorporating 0.5 wt.% rGO are presented in Fig. 14 (a-h). Notably, the fracture surface exhibits a distinctive pattern characterized by the presence of microdimples (Fig. 14g), which are observed to be both tiny and uniformly distributed. The presence of these microdimples is indicative of significant plastic deformation that occurred prior to material rupture, suggesting a ductile fracture mode. Furthermore, Certain rGO particles were observed to be dislodged and pulled out at the edges of tear ridges within the fracture surface. This phenomenon is particularly evident in the magnified images from the interior of these dimples, as illustrated in Figure 14 (e) which is confirmed by EDS in Figure 14 (f, h), The fracture of the rGO particles within these composites is infrequent. This rarity in rGO fracture can be attributed to the remarkable disparity in strength between rGO and the aluminum matrix. Because rGO is much stronger than the aluminum matrix, the main reinforcement mechanism in these composites is the pull out of rGO particles from the aluminum matrix during fracture. This observation provides valuable insights into the mechanical behavior of these composites, emphasizing the reinforcement mechanisms and the enhancements in tensile strength.

CONCLUSIONS

This study is on the synthesis of reduced graphene oxide (rGO) particles prepared from graphite through a modified Hummer's method followed by incorporating within the matrix of A356 alloy using a combination of semisolid stir mixing and squeeze casting. Our objective was to investigate the effect of varying percentages of rGO additions on the mechanical properties and thermal expansion of A356 alloy.

The study led to several significant conclusions:

- It has been possible to incorporate up to 0.75wt.% of rGO particles in the matrix of cast A356 Al-Si alloy using semisolid stir mixing followed by the squeeze casting process.
- Squeeze casting of 0.5 wt.% rGO in the A356 matrix shows a reduction in the dendrite arm spacing compared to the base A356 alloy.
- The CTE of the composites decreased with increasing rGO content. In the temperature range of 50 to 200C (122-392F) at RT-50C, the CTE of the base alloy was 21.7. However, it decreased to 10.8 $\times 10^{-6}$ /°C with the addition of 0.5wt.% rGO.
- The squeeze cast Al 356-0.5%rGO composites after T6 heat treatment had an increase in tensile strength from 260 MPa for A356 alloy to 346 MPa and an increase in hardness from 106 BHN to 130 BHN.

REFERENCES

1. Rohatgi, Pradeep, K. "Metal matrix composites," *Defense science journal* 43.4; 323 (1993).
2. Ajay Kumar, P., Rohatgi, P., & Weiss, D., "50 years of foundry-produced metal matrix composites and future opportunities," *International Journal of Metalcasting*, 14(2), 291-317 (2020).
3. Miracle, D.B., "Metal Matrix Composites–from Science to Technological Significance," *Composites Science and Technology*, vol. 65, issues 15-16: pp. 2526-2540 (Dec 2005).
4. Dasari, B.L., Morshed, M., Nouri, J.M., Brabazon, D., & Naher, S., "Mechanical properties of graphene oxide reinforced aluminium matrix composites," *Composites Part B: Engineering*, 145, 136-144 (2018).
5. Sadeghi, Behzad, and Pasquale Daniele Cavaliere, "Reviewing the Integrated Design Approach for Augmenting Strength and Toughness at Macro-and Micro-Scale in High-Performance Advanced Composites," *Materials*, 16.17:5745 (2023).
6. Kim, D., Nam, S., Roh, A., Yoo, S., Quevedo-Lopez, M., & Choi, H., "Effect of interfacial features on the mechanical and electrical properties

of rGO/Al composites," *Journal of Materials Science*, 52, 12001-12012 (2017).
7. Soltani, T., & Lee, B.K., "A benign ultrasonic route to reduced graphene oxide from pristine graphite," *Journal of colloid and interface science*, 486, 337-343 (2107).
8. Li, Z., Fan, G., Tan, Z., Guo, Q., Xiong, D., Su, Zhang, D., "Uniform dispersion of graphene oxide in aluminum powder by direct electrostatic adsorption for fabrication of graphene/aluminum composites," *Nanotechnology*, 25(32), 325601 (2014).
9. Wang, J., Li, Z., Fan, G., Pan, H., Chen, Z., & Zhang, D., "Reinforcement with graphene nanosheets in aluminum matrix composites," *Scripta Materialia*, 66(8), 594-597 (2012).
10. Shah R., Pai N., Rosenkranz A., Shirvani K., Marian, M., "Tribological behavior of additively manufactured metal components," 6(6):138 (2022).
11. Yolshina, L.A., Muradymov, R.V., Korsun, I.V., Yakovlev, G.A., & Smirnov, S.V., "Novel aluminum-graphene and aluminum-graphite metallic composite materials: Synthesis and properties," *Journal of alloys and compounds*, 663, 449-459 (2016).
12. Hanifah, M.F.R., Jaafar, J., Aziz, M., Ismail, A.F., Rahman, M.A., & Othman, M.H.D, "Synthesis of graphene oxide nanosheets via modified hummers' method and its physicochemical properties," *Jurnal Teknologi*, 74(1), 189-192 (2015).
13. Saini, A., Kumar, A., Anand, V.K., Sood, S.C., "Synthesis of graphene oxide using modified Hummer's method and its reduction using hydrazine hydrate," 40(2):67-71 (2016).
14. Agarwal, V., & Zetterlund, P.B., "Strategies for reduction of graphene oxide–A comprehensive review," *Chemical Engineering Journal*, 405, 127018 (2021).
15. Lavin-Lopez, P., Paton-Carrero, A., Sanchez-Silva, L., Valverde J.L., Romero, A. ,"Influence of the reduction strategy in the synthesis of reduced graphene oxide,"*Adv Powder Tech*., 28(12):3195-203 (2017).
16. Korucu, H., "Evaluation of the performance on reduced graphene oxide synthesized using ascorbic acid and sodium borohydride: Experimental designs-based multi-response optimization application," *Journal of Molecular Structure*, 1268, 133715 (2022).
17. Hidayah, N., Liu, W., Lai, C.W., Noriman, N.Z., Khe, C.S., Hashim, U., & Lee, H.C., "Comparison on graphite, graphene oxide and reduced graphene oxide: Synthesis and characterization," *AIP conference proceedings*, Vol. 1892, No. 1 (Oct 2017).
18. Kotchey, G.P.,"Enzyme-catalyzed degradation of carbon nanomaterials," Doctoral Dissertation, University of Pittsburgh, (Aug. 20, 2013).
19. Adel, M., El-Maghraby, A., El-Shazly, O., El-Wahidy, E.W.F., & Mohamed, M.A., "Synthesis of few-layer graphene-like nanosheets from glucose: New facile approach for graphene-like nanosheets large-scale production," *Journal of Materials Research*, 31(4), 455-467 (2016).
20. Aliyev, E., Filiz, V., Khan, M.M., Lee, Y.J., Abetz, C., Abetz, V., "Structural characterization of graphene oxide: Surface functional groups and fractionated oxidative debris," *Nanomaterials*, 9(8), 1180 (2019).
21. Ghalkhani, M., Khosrowshahi, E.M., Sohouli, E., Eskandari, K., Aghaei, M., Rahimi-Nasrabadi, M. & Kouchaki, E., "Electrochemical monitoring of carbamazepine in biological fluids by a glassy carbon electrode modified with CuO/ZnFe2O4/rGO nanocomposite," *Surfaces and Interfaces*, 30, 101943 (2022).
22. Bera, M., & Maji, P.K., "Effect of structural disparity of graphene-based materials on thermo-mechanical and surface properties of thermoplastic polyurethane nanocomposites," *Polymer*, 119, 118-133 (2017).
23. Smith, B.C., "The carbonyl group, part I: introduction," *Spectroscopy*, 32(9), 31-36 (2017).
24. Bera M., Yadav, C., Gupta P, Maji, P.K., "Facile one-pot synthesis of graphene oxide by sonication assisted mechanochemical approach and its surface chemistry, *Journal of Nanoscience and Nanotechnology*, 18(2):902-12 (2018).
25. Cox, J., Luong, D.D., Shunmugasamy, V.C., Gupta, N., Strbik III, O.M., & Cho, K., "Dynamic and thermal properties of aluminum alloy A356/silicon carbide hollow particle syntactic foams," *Metals*, 4(4), 530-548 (2014).
26. Kwon, H., Park, D.H., Silvain, J.F., & Kawasaki, A., "Investigation of carbon nanotube reinforced aluminum matrix composite materials," *Composites Science and Technology*, 70(3), 546-550 (2010).
27. Nyanor, P., El-Kady, O., Yehia, H.M., Hamada, A.S., Nakamura, K., & Hassan, M.A.,"Effect of carbon nanotube (CNT) content on the hardness, wear resistance and thermal expansion of in-situ reduced graphene oxide (rGO)-Reinforced aluminum matrix composites," *Metals and Materials International*, 27, 1315-1326 (2021).
28. Eid, M., Kaytbay, S., Elkady, O., El-Assal, A.,. "Microstructure and mechanical properties of CF/Al composites fabricated by hot coining technique," *Ceramics International,* 47(15):21890-904 (2021).
29. Zhang, Y.H., & Wu, G.H., "Interface and thermal expansion of carbon fiber reinforced aluminum matrix composites," *Transactions of Nonferrous Metals Society of China*, 20(11), 2148-2151 (2010).
30. Guan, R.G., & Tie, D., "A review on grain refinement of aluminum alloys: progresses, challenges and prospects," *Acta Metallurgica Sinica* (English Letters), 30, 409-432 (2017).
31. Li, P., Chen, L., Cao, B., & Shi, K., "Hierarchical microstructure architecture: A roadmap towards strengthening and toughening reduced graphene oxide/2024Al matrix composites synthesized by flake powder thixoforming," *Journal of Alloys and Compounds,* 823, 153815 (2020).

32. Tayyebi, M., & Alizadeh, M., "Thermal and wear properties of Al/Cu functionally graded metal matrix composite produced by severe plastic deformation method," *Journal of Manufacturing Processes*, 85, 515-526 (2023).
33. Zhao, L., Guo, Q., Li, Z., Xiong, D.B., Osovski, S., Su, Y., & Zhang, D., "Strengthening and deformation mechanisms in nanolaminated graphene-Al composite micro-pillars affected by graphene in-plane sizes," *International Journal of Plasticity*, 116, 265-279 (2019).
34. Gao, X., Yue, H., Guo, E., Zhang, H., Lin, X., Yao, L., & Wang, B., "Preparation and tensile properties of homogeneously dispersed graphene reinforced aluminum matrix composites," *Materials & design*, 94, 54-60 (2016).
35. Shin, S.E., Choi, H.J., Shin, J.H., & Bae, D.H., "Strengthening behavior of few-layered graphene/aluminum composites," *Carbon*, 82, 143-151 (2015).
36. Singh, K., Khanna, V., Chaudhary, V., "Effect of hybrid reinforcements on the mechanical properties of copper nanocomposites," *ECS Journal of Solid State Science and Technology*,11(9) (Sept 2022).
37. Chou, S.N., Huang, J.L., Lii, D.F., & Lu, H.H., "The mechanical properties of Al2O3/aluminum alloy A356 composite manufactured by squeeze casting," *Journal of alloys and compounds,* 419(1-2), 98-102 (2006).
38. Li, Zan, Guo, Q., Li, Zhiqiang., Fan, G., Xiong, D-B., Su, Y., Zhang, J., Zhang, D., "Enhanced mechanical properties of graphene (reduced graphene oxide)/aluminum composites with a bioinspired nanolaminated structure," *Nano letters*, 15(12), 8077-8083 (Dec 9, 2015).